

# Neutron Scattering Study of $\text{URu}_{2-x}\text{Re}_x\text{Si}_2$ with $x = 0.10$ : Driving Order towards Quantum Criticality

T. J. Williams,<sup>1</sup> Z. Yamani,<sup>2</sup> N.P. Butch,<sup>3</sup> G.M. Luke,<sup>1,4</sup> M.B. Maple,<sup>3</sup> and W.J.L. Buyers<sup>2,4,\*</sup>

<sup>1</sup>*Department of Physics and Astronomy, McMaster University,  
1280 Main St. W., Hamilton, ON, Canada, L8S 4M1*

<sup>2</sup>*National Research Council, Canadian Neutron Beam Centre,  
Chalk River Laboratories, Chalk River, ON, Canada, K0J 1J0*

<sup>3</sup>*Department of Physics, University of California San Diego, La Jolla, CA, USA, 92093*

<sup>4</sup>*Canadian Institute for Advanced Research, Toronto, Ontario, Canada, M5G 1Z8*

(Dated: May 26, 2022)

We report inelastic neutron scattering measurements in the hidden order state of  $\text{URu}_{2-x}\text{Re}_x\text{Si}_2$  with  $x = 0.10$ . We observe that towards the ferromagnetic quantum critical point induced by the negative chemical pressure of Re-doping, the gapped incommensurate fluctuations are robust and comparable in intensity to the parent material. As the Re doping moves the system toward the quantum critical point, the commensurate spin fluctuations related to hidden order weaken, display a shortened lifetime and slow down. Halfway to the quantum critical point, the hidden order phase survives, albeit weakened, in contrast to its destruction by hydrostatic pressure and by positive chemical pressure from Rh-doping.

PACS numbers: 78.70.Nx, 71.27.+a

In the field of strongly correlated heavy fermion systems, one of the most puzzling long-standing issues is the nature of the hidden order below the large specific heat jump at  $T_0 = 17$  K in  $\text{URu}_2\text{Si}_2$  [1–4]. A superconducting phase also follows below 1.2 K. Despite much research over the past 25 years [5–9] the order parameter remains unknown. The small antiferromagnetic moment of  $0.03 \mu_B$  that develops below 17 K cannot explain the large specific heat jump at this second-order phase transition. Antiferromagnetism therefore cannot be the main cause of the hidden order. The system appears to have condensed into a new phase of matter for which the order parameter and associated symmetries differ from conventional expectations. In previous work, we eliminated crystal fields and orbital currents as a source of hidden order [10, 11]. The spins fluctuating above the 17 K transition are centred on the incommensurate wavevector  $(1 \pm \delta, 0, 0)$  with  $\delta = 0.4$ . Emerging from that wavevector is a high-velocity cone of strongly damped gapless excitations that extend over a finite region of the Brillouin zone. They provide evidence of itinerant, rather than localized spins. In the precursor phase to hidden order, Wiebe *et al.* calculated that these gapless spin fluctuations give rise to a term in the specific heat that closely accounts for the magnitude of the giant specific heat linear in  $T$  that was previously attributed entirely to electrons [11]. In addition, the decrease of the specific heat below  $T_0$  is now understood [11] to arise from the formation of a spin gap below  $T_0$ . More recently, the excitations have been interpreted as the response of itinerant spins to Fermi surface nesting, similar to that of chromium, and specific

nesting vectors were proposed [12]. Evidence of Kondo hybridization arises from STM studies [13]. Despite this considerable progress, the symmetry of the order parameter that condenses in the hidden order phase remains unknown.

Another route to discovering the hidden order symmetry is to move away from the object of interest by applying hydrostatic pressure, or chemical pressure by doping. Hydrostatic pressure has been recently found to cause commensurate condensation of a larger antiferromagnetic moment of  $0.3 \mu_B$  and the collapse of the strong commensurate spin excitations [14, 15]. The hidden order phase is eventually lost with application of pressure beyond about 1.5 GPa. On the contrary, the hidden order phase can be retained by applying negative chemical pressure. This is done by expanding the lattice constants by alloying with rhenium as discovered in the pioneering work of Dalichaouch *et al.* [16, 17]. However, the Re replacement of Ru atoms in  $\text{URu}_{2-x}\text{Re}_x\text{Si}_2$  reduces the hidden order transition from 17 K to 13 K for  $x = 0.10$  [18–20]. It also reduces the superconducting transition from 1.5 K to 0.23 K at  $x = 0.01$ . Interestingly, this represents a first step on the way to reaching a quantum critical point where the hidden order gives over to ferromagnetism [18]. The system exhibits non-Fermi liquid behavior for  $0.15 < x < 0.6$ . The magnetic phase diagram is shown in Fig. 1.

We performed neutron scattering measurements on the DUALSPEC spectrometer at the C5 beamline of the NRU reactor at Chalk River Laboratories. Single crystals of  $\text{URu}_{1.9}\text{Re}_{0.1}\text{Si}_2$  and  $\text{URu}_2\text{Si}_2$  were aligned in the  $(H 0 L)$  scattering plane. Unless otherwise stated, the experiments were performed with a setup and collimation of  $0.53^\circ\text{-PG-}0.55^\circ\text{-S-}0.85^\circ\text{-PG-}1.2^\circ$  with a final scattering energy  $E_f = 14.6$  meV, using two pyrolytic graphite (PG) filters, a vertically focusing PG monochromator and a flat

---

\*author to whom correspondences should be addressed: E-mail:[william.buyers@nrc.gc.ca]

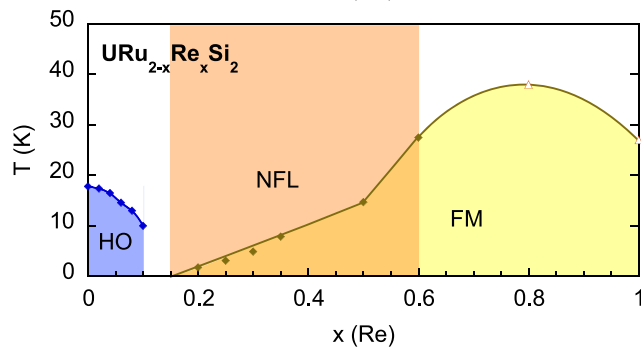


FIG. 1: Magnetic phase diagram of  $\text{URu}_{2-x}\text{Re}_x\text{Si}_2$  showing the antiferromagnetic (hidden order) and ferromagnetic phases. From Ref. [18], also see [19, 20].

PG analyzer. The fast neutron contribution to the background was measured by rotating the analyzer from the Bragg reflection by five degrees.

We find that there is no elastic incommensurate scattering at 2 K at the wavevector  $(1.4\ 0\ 0)$  nor at the commensurate antiferromagnetic point  $(1\ 0\ 0)$ . The latter is in contrast to the parent material, where the weak elastic scattering at the commensurate point is believed to arise from a minority phase [10].

Fig. 2 shows the dependence of scattering along the  $(H\ 0\ 0)$  direction at an energy transfer of 2.9 meV at 2 K and 40 K. This measurement represents the raw data. At 2 K, the scattering shows the relative strength expected from the magnetic form factor at equivalent incommensurate wavevectors  $(0.6\ 0\ 0)$  and  $(1.4\ 0\ 0)$ . At this temperature, the scattering at the commensurate position  $(1\ 0\ 0)$  also exhibits comparable strength. The fast neutron background is shown, as well as the total sample background, obtained from the fitting, described later in the text.

The change in scattering as a function of temperature, both at the commensurate and incommensurate positions, can be used to identify the hidden order transition. At 40 K, well above the hidden order transition, Fig. 2 shows that the incommensurate scattering remains strong, with roughly half the intensity, but the commensurate fluctuations decrease substantially. This is consistent with the suggestion that commensurate  $(1\ 0\ 0)$  dynamic spin excitations are a signature of the hidden order phase [21], whereas the incommensurate scattering is present in both the paramagnetic and hidden order phases. Figure 3 shows the temperature dependence of the commensurate  $(1\ 0\ 0)$  fluctuations at 1.65 meV. This measurement was performed under different experimental conditions, which accounts for the change in the background compared to Fig. 2, but with the same array of single crystals. A discontinuity in the temperature dependence of the peak is observed around  $\sim 13$  K, which may indicate the onset of the hidden order phase. This change is not as clear as that observed in the parent material [21], likely due to electronic disorder associated

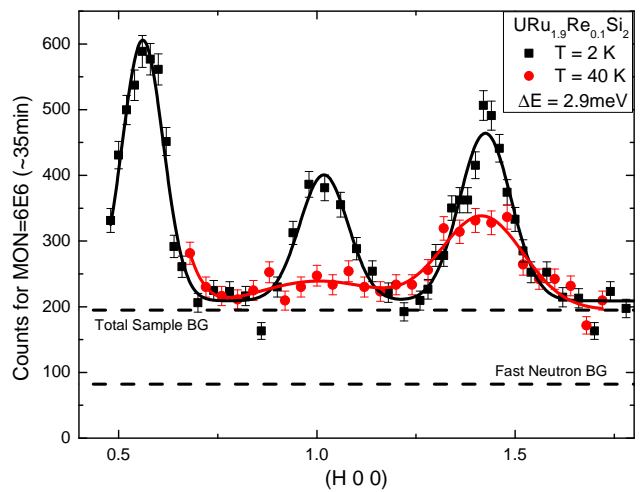


FIG. 2: Inelastic scattering along the  $(H\ 0\ 0)$  direction for an energy transfer of 2.9 meV at  $T = 2$  K (black squares) and  $T = 40$  K (red circles). At 40 K well above the hidden order transition at 17 K, there is partial suppression of the incommensurate fluctuations. In contrast, there is an almost complete suppression of the commensurate fluctuations associated with the hidden order. The lines are Gaussian fits at each of the three peak positions.

with the Re substitution. However, the reduction in this dynamic measure of  $T_0$  is consistent with references [16–18].

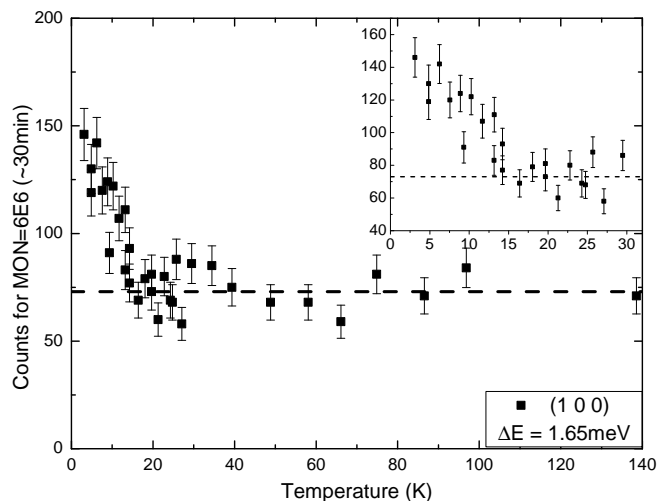


FIG. 3: The temperature dependence of the commensurate  $(1\ 0\ 0)$  fluctuations in  $\text{URu}_{1.9}\text{Re}_{0.1}\text{Si}_2$  at 1.65 meV. A discontinuity in slope is observed at around the onset of the hidden order phase. The inset shows a close-up of the data below 30 K.

Energy scans at  $Q = (1.4\ 0\ 0)$ , comparing the 10% Re-doped with the pure crystal are shown in Fig. 4. The data have been normalized to constant volume for the two crystals via phonon measurements at  $(2.3\ 0\ 0)$  and  $(1.8\ 0\ 0)$  respectively. The spectrum of  $\text{URu}_{1.9}\text{Re}_{0.1}\text{Si}_2$  also

exhibits an incommensurate spin gap similar to that in pure  $\text{URu}_2\text{Si}_2$  [12, 22]. However the gap value is lowered by doping.

The normalized intensity comparison of Fig. 4 shows doping has reduced the intensity at the incommensurate wavevector by a factor of 2 (obtained from the integrated intensity of the peaks). Re-doping also increases the spectral width as seen in Fig. 4, showing that the fluctuations are highly damped by doping. The slowing of fluctuations is more dramatic at the commensurate hidden order wavevector, as shown in Fig. 5. There, the lifetime is so short that the characteristic energy barely gives a peak in the spectrum. It may also signify the destruction of perfect nesting by charge impurities.

The data in Fig. 4 are well-described by the theoretical model of Balatsky [23], given by:

$$\chi^{zz}(\vec{Q}^*, \omega) = A^2 |\Delta_{\vec{Q}^*}|^2 \int \frac{1}{\sqrt{E^2 - \Delta_{\vec{Q}^*}^2}} \frac{1}{\omega^2 - 4E^2} dE \quad (1)$$

to which a constant background (bg) has been added, shown by the blue lines in Fig. 4. The theory is based on a spin resonance in the hidden order state, involving transitions between nested parts of the Fermi surface, separated by  $\vec{Q}^* = (1.4 \ 0 \ 0)$ . This spin resonance is caused by partial Fermi surface nesting which leads to the appearance of a particle-hole condensate [23]. This nesting can occur for a continuous range of wavevectors, from  $(1 \ 0 \ 0)$  to the peak at  $(1.4 \ 0 \ 0)$ , corresponding to the maximum nesting vector between the two Fermi surface pockets proposed from band structure calculations [12, 23]. The fermion energies are assumed to rise quadratically above a hidden order gap  $\Delta_{\vec{Q}^*}$ , allowing pairs of excitations to contribute to the dynamic susceptibility measured by neutron scattering [23]. Thus the gap in the spin spectrum in Fig. 4 is equal to  $2\Delta_{\vec{Q}^*}$ .

In Fig. 4, the models for the spectrum have been convoluted with the 4D instrumental resolution function using Reslib [24]. The required spin velocities in three directions were taken from [22]. The spectrum was broadened slightly to deal with the square root singularity of the Balatsky nesting Ansatz of Eq. 1, by adding a small imaginary part  $\gamma$  to the frequency in such a way that it is analogous to the broadening  $\gamma$  of Fig. 4 described in relation to Eq. 2. The data have been corrected for higher order perturbation of the monitor rate.

Recent measurements of the inelastic scattering along  $(H \ 0 \ 0)$  in the parent compound have been analyzed [21] in terms of a peak and a continuum. In contrast we find that for both the pure and doped systems, the tail to high-energy is well-described by the asymmetry of the Balatsky nesting equation (1) and no additional continuum is needed. We suggest that the doped Re atoms render the nesting less perfect and so allow spin fluctuations over a wider range of energies. This is consistent with the picture of the incommensurate spin resonance that leads to Equation 1.

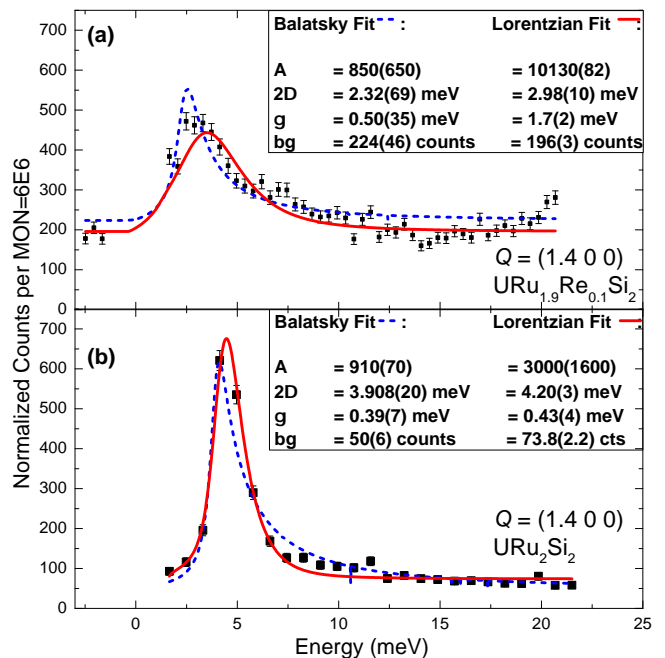


FIG. 4: (color online) The fits to the incommensurate fluctuations (a) for  $\text{URu}_{1.9}\text{Re}_{0.1}\text{Si}_2$  at  $T = 2$  K and (b) for pure  $\text{URu}_2\text{Si}_2$  at  $T = 3$  K and 5 K (combined data). The blue line is the fit to Eq. 1 and the red line is a fit to a Lorentzian of energy  $2\Delta$ , amplitude  $A$  and damping  $2\gamma$ =FWHM, convoluted with the resolution function, as described in the text. For the Re-doping, the nesting gap energy,  $\Delta$ , is reduced to 60% of its value in the pure system.

Attempts to fit the commensurate fluctuations at  $(1 \ 0 \ 0)$  to the Balatsky theoretical model did not converge. The data for the commensurate and incommensurate excitations for both doped and pure compounds were therefore fitted to Lorentzians for comparison purposes, given by:

$$I(\vec{Q}^*, \omega) = \frac{A}{\omega_{\vec{Q}^*}} \cdot \left[ \frac{1}{(\omega - \omega_{\vec{Q}^*})^2 + \gamma^2} - \frac{1}{(\omega + \omega_{\vec{Q}^*})^2 + \gamma^2} \right] \quad (2)$$

This was multiplied by a Bose factor, and convoluted with the resolution function, as described above. The commensurate fluctuations at  $(1 \ 0 \ 0)$  for the Re-doped and parent samples are shown in Fig. 5(a) and Fig. 5(b), respectively. The resolution conditions for the  $(1 \ 0 \ 0)$  energy scan (Fig. 5(a)) were slightly different, with a setting of  $0.53^\circ$ -PG- $0.48^\circ$ -S- $0.55^\circ$ -PG- $1.2^\circ$ . Compared to the parent compound with a spin gap of 1.75 meV, the commensurate fluctuations are peaked at a lower energy of 1.38 meV, a reduction of 72%, which tracks the reduction of  $T_0$ . Within a nesting picture, it appears that the Re impurities (chemical pressure) greatly weaken the nesting present in the pure system.

As temperature is increased, the commensurate fluctuations are destroyed much more quickly than are the

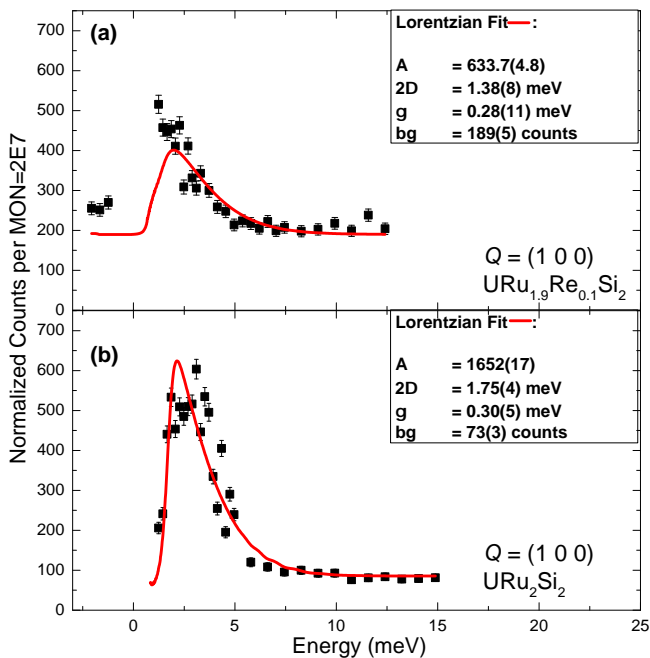


FIG. 5: (color online) (a) The inelastic scattering at  $(1\ 0\ 0)$  in the  $\text{URu}_{1.9}\text{Re}_{0.1}\text{Si}_2$  sample, measured at  $T = 2$  K. (b) The  $(1\ 0\ 0)$  inelastic scattering in the pure  $\text{URu}_2\text{Si}_2$  system, measured at  $T = 3$  K and 5 K (combined data). Both were fit to a Gaussian for the elastic scattering, and a Lorentzian of energy  $\omega_{\vec{Q}^*} = 2\Delta$ , amplitude  $A$  and damping  $2\gamma = \text{FWHM}$  for the inelastic peak, convoluted with the resolution function. The commensurate fluctuations of the hidden order phase are damped in the presence of Re-doping.

incommensurate fluctuations at  $(1.4\ 0\ 0)$ . Thus the hidden order gap for  $(1\ 0\ 0)$  antiferromagnetic fluctuations becomes less well defined. Both the commensurate (Fig. 5(a)) and incommensurate (Fig. 4(a)) spectral form is that of a resonant frequency that decays into the Re-induced continuum of the itinerant particle-hole states. The Re doping achieves this, we suggest, by  $\vec{Q}$ -broadening of the nesting that gave the well-defined spectral onset above the gap in the pure hidden order system  $\text{URu}_2\text{Si}_2$ . The relatively large spin velocities [22] then convert the  $\vec{Q}$ -broadening into the observed spectral broadening. Our results suggest that the gap may vanish when the quantum phase transition to ferromagnetism is reached.

We also studied the width in wavevector of the column of spin fluctuations that emerges from the incommensurate points. Constant-energy scans were measured along  $(H\ 0\ 0)$  at energies ranging from 2.1 meV to 10.3 meV as shown in Fig. 6. These  $\vec{Q}$ - $E$  patterns with Re present are very similar to those observed in the pure material [12]. The FWHM in  $H$  at 10 meV is anomalously large because of overlap with spin cones emanating from  $(1\ 0\ 0)$  and phonons from  $(2\ 0\ 0)$ , but the low-energy correlation width is accurate. We note that the intensity and peak energy of the excitations have decreased from the parent material, but their  $\vec{Q}$ -width and hence dynamic

spin correlation lengths remains unchanged. Thus those incommensurate fluctuations that are not a primary signature of hidden order like those around  $(1.4\ 0\ 0)$  are little affected by doping or by temperature. Thereby, the predominant behaviour that survives the approach to the quantum critical point is the robust cone of gapped incommensurate fluctuations, similar to the pure material.

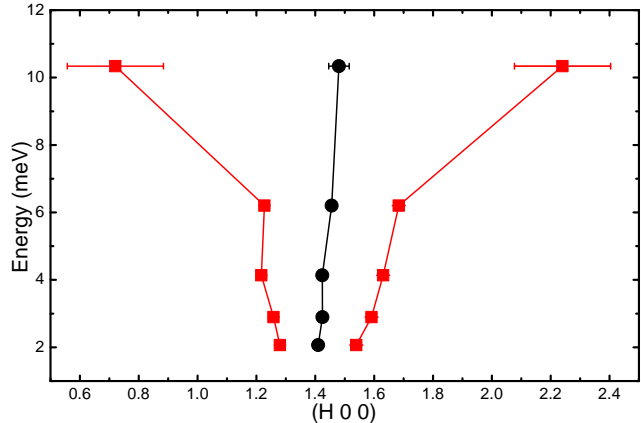


FIG. 6: Locus of the half widths in reduced wavevector  $H$  of spin fluctuations around  $(1.4\ 0\ 0)$ . These inverse dynamic correlation lengths are narrow in wavevector for low energies, but broaden dramatically at higher energies. The black vertical line shows the centroid of the scattering arising from a column of itinerant excitations in the  $E$ - $\vec{Q}$  plane. The error bars for low energy fits lie within the symbol size.

Our results demonstrate that the commensurate spin fluctuations lose much of their collective peaking as nesting is disturbed by approach to the presumed ferromagnetic [20] quantum critical point. In addition, we find that the lifetime of the spin fluctuations, or more likely the fermions from which they arise, are shorter in the Re-doped compound. The observation of a commensurate spin gap indicates that the hidden order phase survives at least half-way to the quantum critical point albeit in a weakened form. Our neutron results therefore show that the effect of Re doping, in contrast to the antiferromagnetic enhancement and hidden order destruction by Rh-doping[18, 19], is to weaken, but surprisingly, not to destroy the hidden order on approach to the quantum phase transition to ferromagnetism. This is consistent with the part of the hidden order phase boundary inferred from specific heat measurements [19, 20].

### Acknowledgments

We appreciate the hospitality and support of the NRC Canadian Neutron Beam Center at Chalk River laboratories and the technical support of R. Sammon. Research at McMaster University is supported by NSERC. Research at UCSD was supported by the U.S. Department of Energy under Grant Number DE-FG02-04ER46105.

- 
- [1] T.T.M. Palstra, A.A. Menovsky, J. van den Berg, A.J. Dirkmaat, P.H. Kes, G.J. Nieuwenhuys and J.A. Mydosh. *Phys. Rev. Lett.* **55**, 2727 (1985).
- [2] M.B. Maple, J.W. Chen, Y. Dalichaouch, T. Kohara, C. Rossel, M.S. Torikachvili, M.W. McElfresh and J.D. Thompson. *Phys. Rev. Lett.* **56**, 185 (1986).
- [3] W. Schlabitz, J. Baumann, B. Pollit, U. Rauchschwalbe, H.M. Mayer, U. Ahlheim and C.D. Bredl. *Z. Phys. B* **62**, 171 (1986).
- [4] C. Broholm, J.K. Kjems, W.J.L. Buyers, P. Matthews, T.T.M. Palstra, A.A. Menovsky and J.A. Mydosh. *Phys. Rev. Lett.* **58**, 1467 (1987).
- [5] D.A. Bonn, J.D. Garrett and T. Timusk. *Phys. Rev. Lett.* **61**, 1305 (1988).
- [6] W.J.L. Buyers, Z. Tun, T. Peterson, T.E. Mason, J.-G. Lussier, B.D. Gaulin and A.A. Menovsky. *Physica B* **199&200**, 95 (1994).
- [7] T.E. Mason, W.J.L. Buyers, T. Peterson, A.A. Menovsky and J.D. Garrett. *J. Phys.: Condens. Matter* **7**, 5089 (1995).
- [8] F. Bourdarot, A. Bombardi, P. Burlet, M. Enderle, J. Flouquet, P. Lejay, N.Kernavanois, V.P. Mineev, L.Paolasini, M.E. Zhitomirsky and B. Fåk. *Physica B* **359-361**, 986 (2005).
- [9] P. G. Niklowitz, S. R. Dunsiger, C. Pfeleiderer, P. Link, A. Schneidewind, E. Faulhaber, M. Vojta, Y.-K. Huang, J. A. Mydosh, arXiv:1110.5599.
- [10] C.R. Wiebe, G.M. Luke, Z. Yamani, A.A. Menovsky and W.J.L. Buyers. *Phys. Rev. B* **69**, 132418 (2004).
- [11] C.R. Wiebe, J.A. Janik, G.J. MacDougall, G.M. Luke, J.D. Garrett, H.D. Zhou, Y.-J. Jo, L. Balicas, Y. Qiu, J.R.D. Copley, Z. Yamani and W.J.L. Buyers. *Nature Physics* **3**, 96 (2007).
- [12] J.A. Janik, H.D. Zhou, Y.-J. Jo, L. Balicas, G.J. MacDougall, G.M. Luke, J.D. Garrett, K.J. McClellan, E.D. Bauer, J.L. Sarrao, Y. Qiu, J.R.D. Copley, Z. Yamani, W.J.L. Buyers and C.R. Wiebe. *J. Phys.: Condens. Matter* **21**, 192202 (2009).
- [13] A.R. Schmidt, M.H. Hamidian, P. Wahl, F. Meier, A.V. Balatsky, J.D. Garrett, T.J. Williams, G.M. Luke and J.C. Davis. *Nature* **465**, 570 (2010).
- [14] D. Aoki, F. Bourdarot, E. Hassinger, G. Knebel, A. Miyake, S. Raymond, V. Taufour and J. Flouquet. *J. Phys. Soc. Jap.* **78**, 053701 (2009).
- [15] A. Villaume, F. Bourdarot, E. Hassinger, S. Raymond, V. Taufour, D. Aoki and J. Flouquet. *Phys. Rev. B* **78**, 012504 (2008).
- [16] Y. Dalichaouch, M.B. Maple, M.S. Torikachvili and A.L. Giorgi. *Phys. Rev. B* **39**, 2423 (1989).
- [17] Y. Dalichaouch, M.B. Maple, J.W. Chen, T. Kohara, C. Rossel, M.S. Torikachvili and A.L. Giorgi. *Phys. Rev. B* **41**, 1829 (1990).
- [18] N.P. Butch and M.B. Maple. *J. Phys.: Condens. Matter* **22**, 164204 (2010).
- [19] N.P. Butch and M.B. Maple. *Phys. Rev. Lett.* **103**, 076404 (2009).
- [20] E.D. Bauer, V.S. Zapf, P.-C. Ho, N.P. Butch, E.J. Freeman, C. Sirvent and M.B. Maple. *Phys. Rev. Lett.* **94**, 046401 (2005).
- [21] F. Bourdarot, E. Hassinger, S. Raymond, D. Aoki, V. Taufour, L.-P. Regnault and J. Flouquet. *J. Phys. Soc. Jap* **78**, 064719 (2010).
- [22] C. Broholm, H. Lin, P.T. Matthews, T.E. Mason, W.J.L. Buyers, M.F. Collins, A.A. Menovsky, J.A. Mydosh and J.K. Kjems. *Phys. Rev. B* **43**, 12809 (1991).
- [23] A.V. Balatsky, A. Chantis, H.P. Dahal, D. Parker and J.X. Zhu. *Phys. Rev. B* **79**, 214413 (2009).
- [24] A. Zheludev: ResLib 3.4 (Oak Ridge National Laboratory, 2007).